Breaking the Single-Cycle Barrier

Generation of 1.6 fs pulses opens the gateway to a new regime of nonlinear optics and coherent control.

Miroslav Shverdin, David Walker, Deniz Yavuz, Sunil Goda, G. Y. Yin, Steve Harris.

BOX: Why Generate Single-Cycle Pulses?

Recently, we synthesized ultrawide bandwidth optical pulses, which have the shortest duration ever achieved using optical frequencies, 1.6 fs, and a repetition rate of 11 fs. These pulses are single-cycle, consisting of a single electrical field oscillation, and have over one megawatt of peak power. In addition, we were able to vary the shape of the pulse to generate different prescribed waveforms.

Scientists strive to control various chemical and biological interactions by applying laser pulses of different shapes [1-3]. A system can be forced into certain states based on the shape of the applied electric field. In the optical regime, however, the shortest pulses produced to date (~ 4 fs) cover less than one octave of bandwidth, which limits the possible types of waveforms that can be produced. (An octave is an interval of frequencies where the ratio of the highest to the lowest is 2:1.)

Synthesis of arbitrarily shaped multi-octave pulses opens a new frontier of nonlinear optics and coherent control. To obtain full control over a molecular reaction, we need to match the bandwidth of the pulse with the full molecular spectrum. The spectra of most molecular materials span a wide range of frequencies, and now we can simultaneously access that entire range with our source. We envision novel applications of multi-octave pulses for coherent control of chemical reactions, as a probe for ever-shorter physical processes, and for highly efficient generation of far infra-red and vacuum ultra-violet radiation.

Introduction

From Fourier theory, we know that any periodic shape can be formed by combining sinusoidal waves with prescribed amplitudes, frequencies, and relative phases. Functions such as a square-wave, or a sawtooth-wave require a range of frequencies covering several octaves of bandwidth. In the acoustic regime, multi-octave radiation sources are abundant. A typical concert piano spans 7 octaves of bandwidth. The voice of a good opera singer can stretch over nearly 4 octaves. In optics, a laser is a source of coherent, intense, monochromatic radiation, with a sinusoidal electric field. In this article, we describe a unique source of laser radiation, developed in our group over the last several

years, that spans over 4 octaves of bandwidth (from 195 nanometers to 3 microns) and consists of over 200 discrete frequency components.

We also describe our latest pulse shaping experiment. We have achieved phase control over 7 spectral components stretching from 410 nm to 1.56 microns (2 octaves). By changing the relative phases of these seven sidebands, we have synthesized a train of 1.6 fs pulses with a period of 11 fs. These pulses are single-cycle, consisting of one electric field oscillation under the envelope. We have also synthesized a frequency modulated pulse, where the electric-field chirp is apparent over three field oscillations.

Spectrum generation

Ultrashort pulse generation requires a wide-bandwidth coherent spectrum. An **incoherent** radiation source, such as sunlight, a high pressure arc lamp, or an atomic line emission lamp consists of many spectral components all having randomly varying phases. The time structure from such a source is simply white noise. A **coherent** light source has a fixed phase relation among the different spectral components, which interfere to produce well-defined waveforms.

It is well-known that an electrooptic modulator can phase modulate an applied laser field to produce sidebands at new frequencies. These modulators, based on electrooptic crystals, have low conversion efficiencies and typical bandwidths around 1 GHz. Our group has developed a process using molecular modulation that has unity conversion efficiency and a modulation bandwidth of 90 THz [4]. This method involves exciting a vibrational or a rotational mode of a molecule using two intense laser fields. Classically, we can picture this interaction as driving a harmonic oscillator near its resonance at the beat note frequency of the two lasers. In this manner, we prepare a very efficient molecular modulator. The resulting molecular motion mixes with the two applied fields to produce new coherent frequencies.

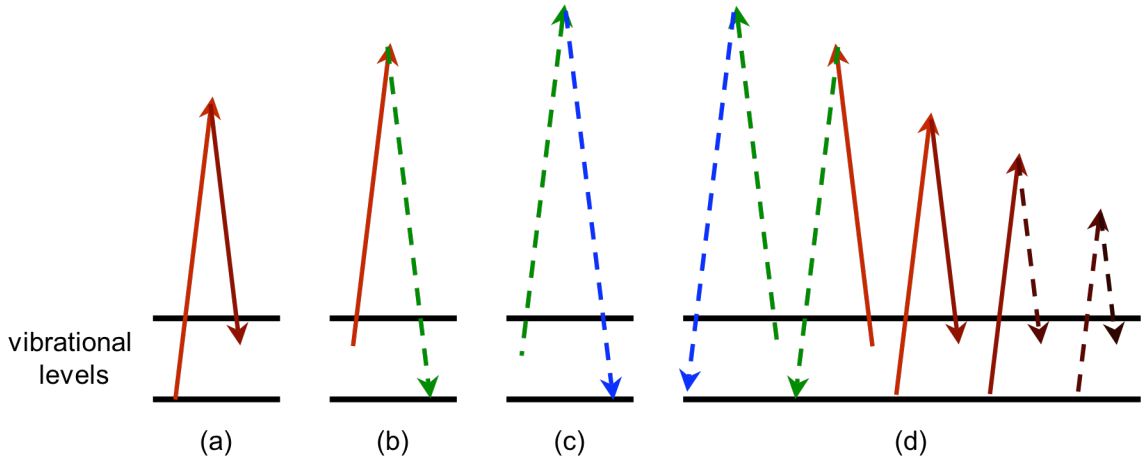

Fig. 1: (a) The pump (red) and Stokes (dark red) driving lasers drive a molecular vibrational transition slightly off resonance.

(b) The pump laser then mixes with the molecular vibration to generate an additional anti-Stokes frequency (broken green line).
(c) The anti-Stokes field (broken green line), in turn, mixes with the molecular vibration to generate the next anti-Stokes frequency (broken blue line).
(d) This generation process continues as described to generate both new Stokes (broken lines to the left of solid lines) and anti-Stokes (broken lines to the right of solid lines) frequencies. The number of new frequencies depends on the efficiency of the process.

If many efficient electrooptic modulators with different modulation frequencies are cascaded in series, then the total number of produced sidebands will be the product of the number of sidebands that each modulator would produce by itself. To produce over 200 sidebands, we simultaneously excite a vibrational transition in deuterium and a rotational transition in hydrogen using two pairs of lasers. The experimental realization of this effect is shown in Fig. 2.

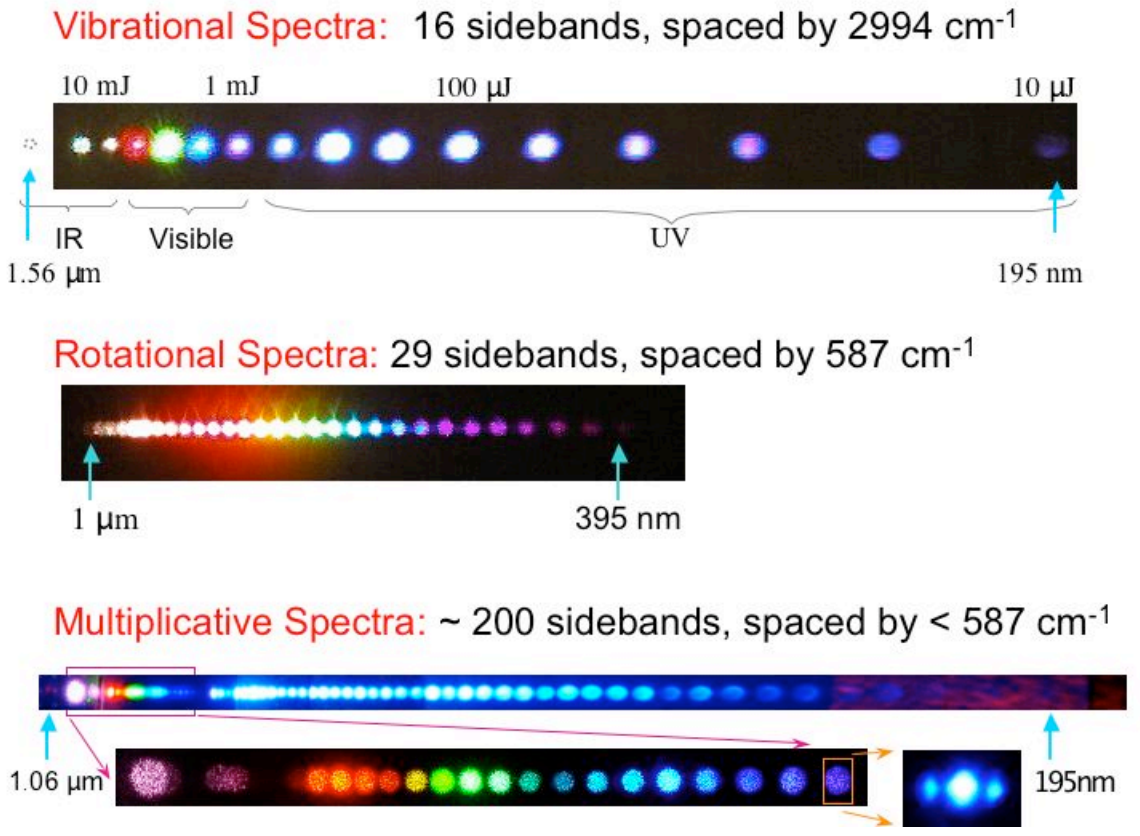

Fig 2: Three different spectra. The first is obtained by driving a vibrational transition in D_2. The second by driving a rotational transition in H_2. The third spectrum is obtained by simultaneously driving both transitions (cascading the two modulators).

When we excite a fundamental vibrational transition in deuterium, we generate an additional 14 sidebands (Fig. 2a) [4]. When we excite a single rotational transition in hydrogen, we produce in excess of 27 sidebands (Fig. 2b) [5]. If we simultaneously drive both transitions, then we obtain the multiplicative spectrum (Fig. 2c) [6]. We can picture this process as cascading a vibrational and a rotational modulator. Here, the total number of observed frequencies is approximately one-half the product of the rotational and vibrational number of sidebands. This happens because the additional sidebands are generated at such low efficiency that they are not resolved.

Due to the experimental difficulties of simultaneously controlling the phases of so many sidebands, we used a single vibrational modulator in our pulse shaping experiment. The vibrational spectrum (Fig. 2a) is obtained by applying two Q-switched lasers. One is a Nd:YAG diode-seeded laser at 1064 nm with a pulse energy of 70 mJ and a pulse duration of 10 ns. The second is a homemade Ti:Sapphire ring-cavity laser at 807 nm. It produces transform-limited 15 ns pulses with 60 mJ of energy. This laser is seeded by a tunable diode laser and is pumped by the second harmonic of a separate Nd:YAG laser. The D_2 molecules are contained inside a liquid nitrogen cooled, 50 cm long cell at a pressure of 60 torr. The gas cell is cooled to reduce the thermal population of upper energy levels and decrease the Doppler linewidth. The output after the deuterium cell appears as white light. The generated sidebands are observed after dispersing the beam with a prism.

After the cell exit window, the relative phases of individual sidebands are unknown. To synthesize a prescribed temporal shape, we must adjust the phases of each spectral component, compensating for all dispersive elements in the system [6,7].

Dispersion Control

Due to technical limitations, we work with a seven-sideband subset of the vibrational spectrum, from 410 nm to 1560 nm. The energy of the different components ranges from 2 mJ at 1560 nm to 0.5 mJ at 410 nm. Phase adjustment is done with a liquid crystal spatial light modulator (SLM). The SLM consists of 640 pixels, each measuring 97 microns by 7 mm, spaced 3 microns apart. Each pixel consists of long birefringent molecules inside two clear electrodes. The electrodes allow independent electric fields to be applied in the z-direction to each pixel. As the voltage is applied, the molecules rotate, changing the refractive index. By first calibrating the SLM, we can adjust the phase of each sideband by applying a specified voltage to each pixel.

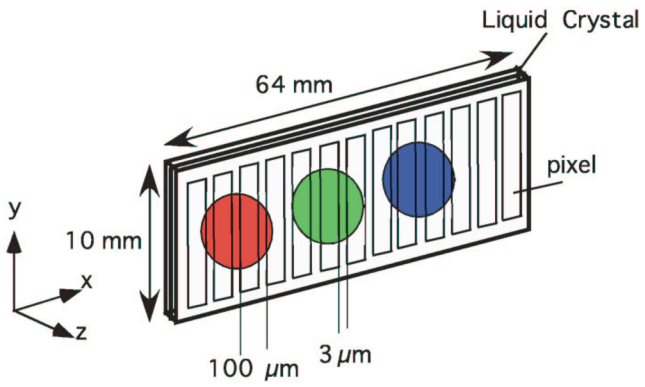

Fig. 3: Liquid crystal spatial light modulator

After the deuterium cell, the seven generated sidebands are dispersed and collimated using two fused silica prisms. All other frequencies are blocked. After collimation, each sideband passes through a range of pixels of the SLM. The beams are then recombined using another prism pair that mirrors the dispersing prism pair. The recombined beam is steered and focused into a xenon chamber. The desired pulse is synthesized in this focal region of overlapping sidebands, inside the Xe chamber. The phase adjustment compensates for Gouy phase shift and all of the optics prior to the focal spot. The ultrashort pulses exist only inside the Xe chamber. Before and after the relative phases are not known.

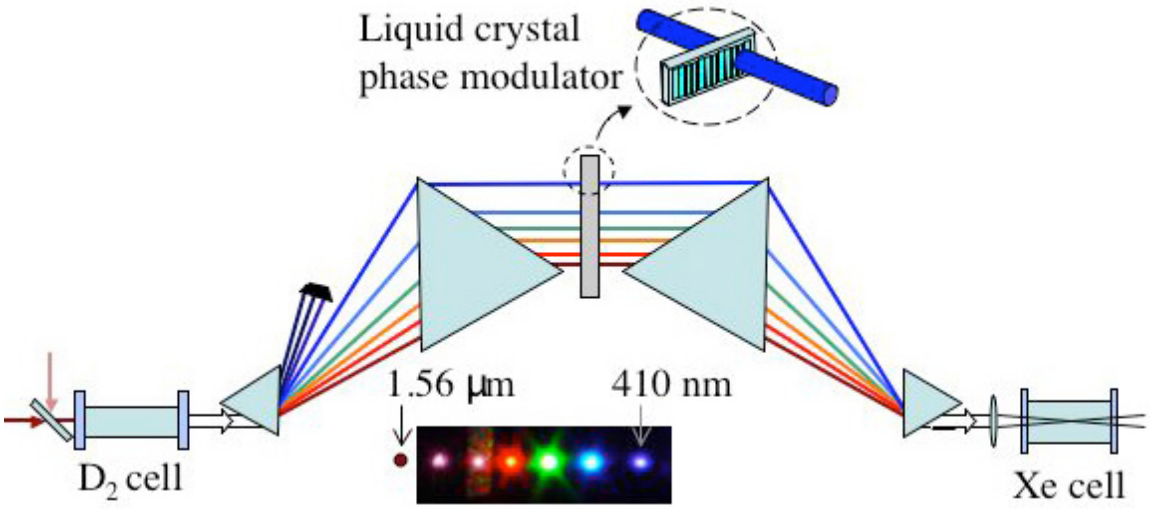

Fig 4: The phase of each of the seven sidebands is adjusted in the phase modulator to produce the desired pulse in the Xe cell. [8]

Four-wave mixing inside the Xe chamber serves as a pulse shape diagnostic, which enables us to properly adjust the individual phases of the seven Raman sidebands. Focusing the sidebands into a Xe chamber produces a very weak UV signal (in the range

of picojoules) at several discrete frequencies. This signal results from the four-wave mixing nonlinear process in xenon. The magnitude of this signal depends on the intensity of the synthesized pulse. Since the shortest possible pulse that can be synthesized also has the highest possible intensity, we adjust the individual phases to maximize the UV signal. In this manner, the UV signal serves as feedback for adaptive phase adjustment by the SLM.

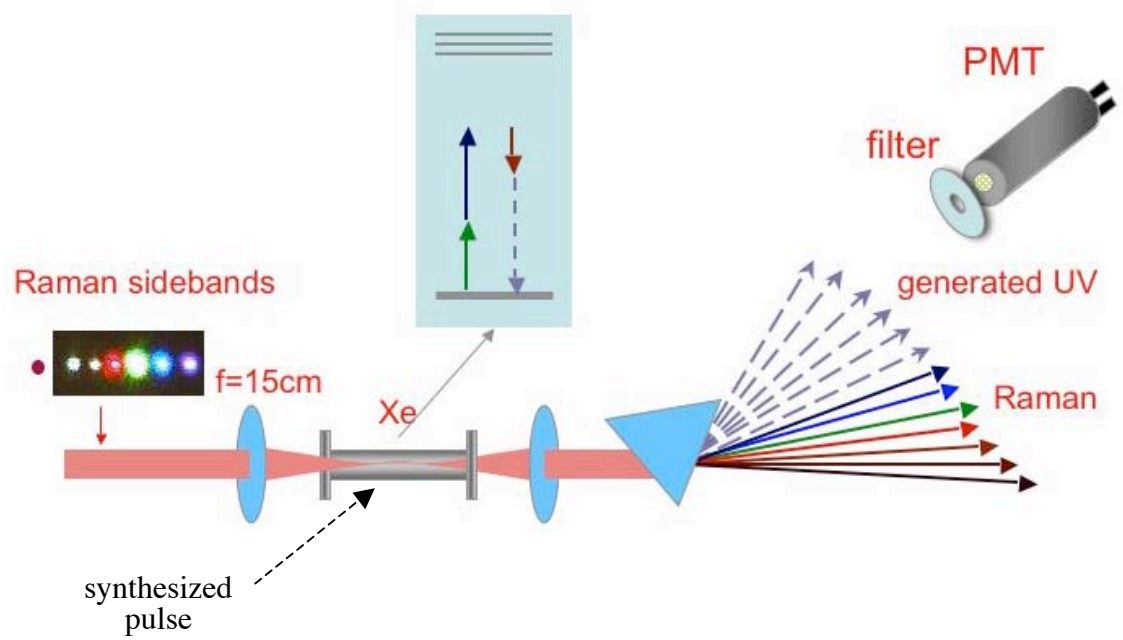

Figure 5: Four-wave mixing detector

Four-wave Mixing in Xenon

Four-wave mixing up-converts the Raman frequencies into the UV. In a typical four-wave process, three different wavelengths are combined in a nonlinear medium. This generates a new frequency equal to some combination of the three input frequencies, as shown in Figure 6.

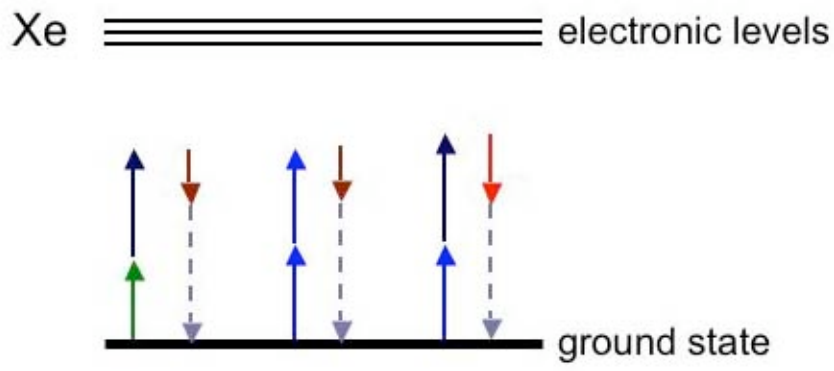

Figure 6: Four-wave mixing. Multiple 3-photon paths of Raman frequencies (solid lines) results in the same generated UV frequency (dashed line). The overall UV signal depends on the phases between the different 3-photon paths.

In our experiment, we focus tightly into the xenon chamber with an f=15 cm lens. In this limit, where the medium is much larger than the confocal parameter, the phase-matching conditions produce radiation whose frequency equals the sum of frequencies of any two Raman sidebands minus a third. Mixing the seven Raman sidebands (which are equally spaced by 90 THz) generates six new UV frequencies, from 365 nm to 236 nm, at efficiencies of 10^{-8} or less. The energy at each UV frequency depends on the relative phases of the Raman sidebands [8].

The weak UV signal is measured using a solar-blind photomultiplier tube. Because of the very low conversion efficiency to the UV, great care is necessary to attenuate the background radiation. The photomultiplier is placed ~2 meters away from the xenon chamber. With a fused silica prism, we spatially separate each of the UV components from its neighbors by ~10 cm. The scattering of the Raman sidebands from various optical components still results in a very poor signal-to-noise ratio. Finally we use an interference filter with a 1000:1 rejection ratio. This combination of the photomultiplier responsivity, beam separation, and filtering results in signal-to-noise ratio of ~1000:1.

Pulse Characterization

Once the ultrashort train of pulses is synthesized, we want to observe and characterize it. Pulses shorter than a few tens of picoseconds cannot be measured directly. Instead, we use indirect correlation methods where part of the pulse is delayed and then combined with the rest of the pulse. By measuring the resulting signal as a function of the delay, we can infer the pulse duration. This type of pulse measurement requires a nonlinear detector. We use four-wave mixing in xenon, which is a third-order process, as the nonlinear detector. Hence, the four-wave mixing serves as both a diagnostic for pulse synthesis and to characterize the pulse shape.

We characterize the synthesized waveform by electronically delaying the pulse formed by three of the Raman sidebands with respect to the pulse formed by the remaining four

Raman sidebands. The synthesized single-cycle waveform can be viewed as the sum of the waveforms formed from these two sets of the interleaving Raman sidebands. Both trains of pulses have nearly the same pulsewidth and half the pulse spacing as the total waveform. The delay of one pulse train with respect to the other is achieved by adding to each of its three sidebands a phase proportional to the sideband's frequency.

At each delay interval between the two pulses, we measure the resulting UV signal at one of the UV frequencies. In Figure 7, the red dots represent the UV energy at 329 nm as a function of the delay [8]. The dashed line is the corresponding theoretical plot of the interaction. This plot is the cross-correlation of the two pulses. It has a period of 5.5 fs (one-half the actual pulse spacing) and cross-correlation width of several femtoseconds. From the agreement between theory and experiment, we conclude that in the synthesized pulse, all the relative phases are the same. The actual synthesized electric field is then shown in Figure 8a.

The electric field is obtained by summing the seven sinusoidal terms at the frequency f_n with the corresponding measured field amplitude, A_n: $E(t) = \sum_{n=1}^{7} A_n \sin(2\pi f_n t + \phi_n)$. Since the phase of each term is the same, we can take $\phi_n = 0$.

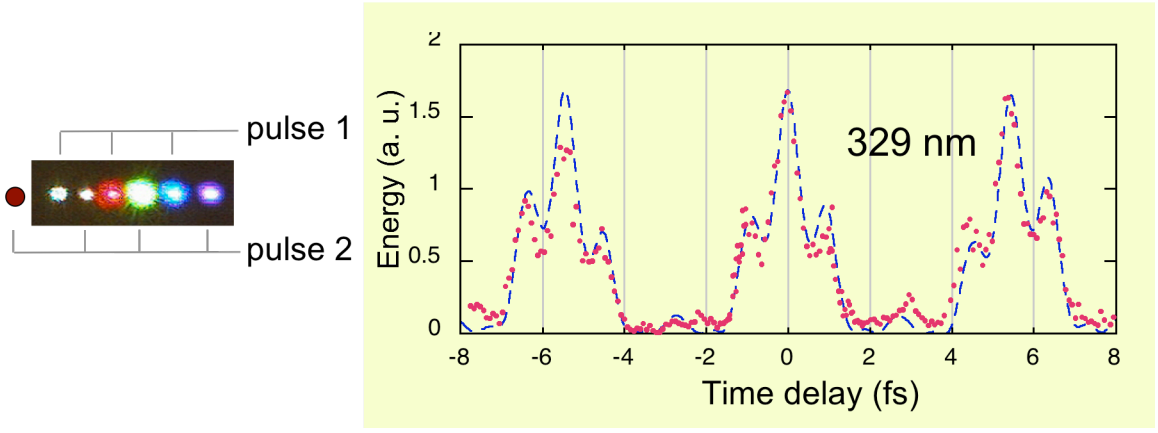

Figure 7: Cross-correlation trace. The cross correlation trace is obtained by electronically delaying pulse 1 with respect to pulse 2. Pulse 1 consists of odd Raman sidebands; pulse 2 consists of even Raman sidebands, as shown.

The synthesized pulses

Because we know the frequencies and relative amplitudes of each of the seven sidebands, we can plot the electric field. The resulting waveform, shown in Figure 8, it has a period of 11 fs [8]. This is due to the discreteness of the spectral sidebands. Pulse separation is inversely proportional to the separation of the adjacent frequencies
(i. e. 1/90 THz = 11 fs). Also, note that the electric field changes in phase from one pulse to the next. This phenomenon, termed a carrier-envelope slip, is caused by the incommensurate frequency comb. In the spectrum, the frequency difference between

adjacent sidebands is not an integer multiple of any one sideband. When the peak electric field coincides with the intensity envelope, the pulse is termed a "cosine pulse." When the peak electric field is offset by $\pi/2$, the pulse is termed a "sine pulse." The pulsewidth of the cosine pulses is 0.5 fs. Each synthesized pulse has a peak power of over 1 MW. There are approximately 10^6 individual pulses under the 10 ns envelopes of the Q-switched pump lasers.

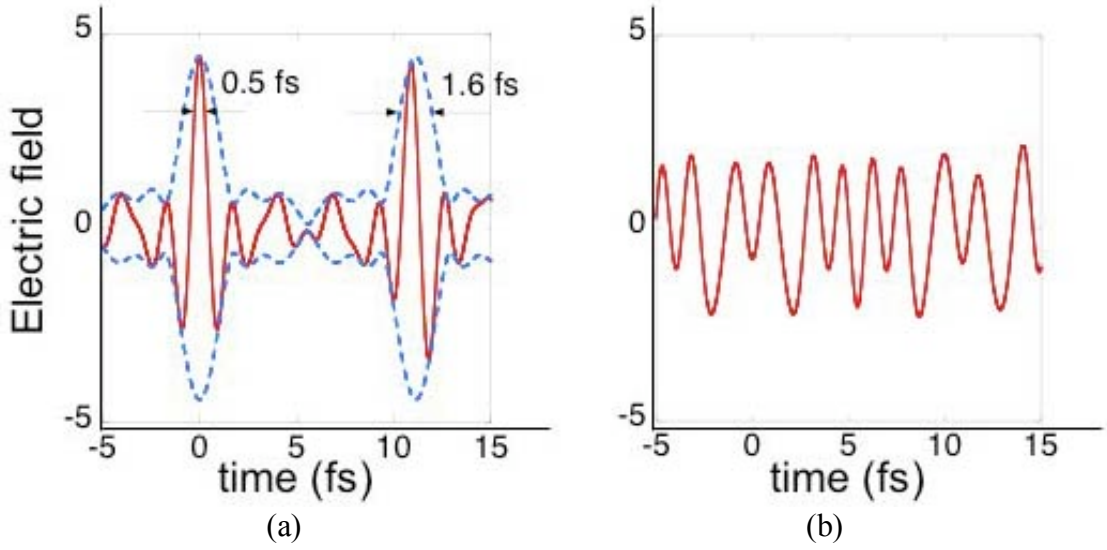

Fig. 8: Synthesized waveforms. (a) Single-cycle and (b) frequency-modulated waveforms

In addition to the single-cycle pulse, we also synthesize a frequency-modulated waveform. After the UV signal is maximized, we conclude that all the relative phases of the Raman sidebands are the same. We can then calculate and add phases to some of the seven sidebands to minimize the generated UV signal. The resulting electric field then corresponds to an FM-like pulse. In all cases, the phase stability is extremely good. We notice no detectable phase drift among the sidebands during several hours of operation.

Future goals

Having achieved phase control over such a wide bandwidth source, we are working on both its applications to a real system and further source improvements. To demonstrate shaping of an arbitrary pulse, we need to extend phase control over a larger bandwidth and to increase the number of spectral components that we simultaneously control.

We are also researching systems where the use of multi-octave optical pulses provides a clear advantage over the narrower bandwidth sources. Another one of our goals is to

attain stop-motion photography of molecular movement [9]. We believe that our multioctave source is a unique tool that, with time, will find many novel applications.

The authors thank Alexei Sokolov for field opening contributions in the area of this work. This work was supported by the U.S. Air Force Office of Scientific Research, the U.S. Army Research Office, and the U.S. Office of Naval Research.

References:

1. T. Brixner, N. H. Damrauer, and G. Gerber, Femtosecond quantum control. *Advan. Atom. Opt. Phys.* **46**, 1–54 (2001).
2. R. Bartels, S. Backus, E. Zeek, L. Misoguti, G. Vdovin, I. P. Christov, M. M. Murnane, and H. C. Kapteyn, Shaped-pulse optimization of coherent emission of high-harmonic soft Xrays. *Nature* 406, 164–166 (2000).
3. B. J. Pearson, J. L. White, T. C. Weinacht, and P. H. Bucksbaum, Coherent control using adaptive learning algorithms. *Phys. Rev. A.* **63**, 063412 (2001).
4. A.V. Sokolov, D.R. Walker, D.D. Yavuz, G.Y. Yin, and S.E. Harris, Raman Generation by Phased and Antiphased States. *Phys. Rev. Lett.* **85,** 562 (2000).
5. D.D. Yavuz, D.R. Walker, G.Y. Yin, and S.E. Harris, Rotational Raman generation with near-unity conversion efficiency. *Opt. Lett.* **27,** 769 (2002)
6. D. D. Yavuz, D. R. Walker, M. Y. Shverdin, G. Y. Yin, and S. E. Harris, Quasiperiodic Raman Technique for Ultrashort Pulse Generation. *Phys. Rev. Lett.* **91**, 233602 (2003).
7. A.V. Sokolov, D.R. Walker, D.D. Yavuz, G.Y. Yin, and S.E. Harris, Femtosecond Light Source for Phase-Controlled Multiphoton Ionization. *Phys. Rev. Lett.* **87**, 033402 (2001).
8. M. Y. Shverdin, D. R. Walker, D. D. Yavuz, G. Y. Yin, and S. E. Harris, Generation of a single-cycle optical pulse. *Phys. Rev. Lett.* **94,** 033904 (2005).
9. A. V. Sokolov, Single-cycle optical pulses synchronized with molecular oscillations Appl. Phys. B **77**, 343 (2003)

About the authors

Miroslav Shverdin is a Postdoc at Stanford University,
David Walker is a Postdoc at Stanford University,
Deniz Yavuz is now a Postdoc at the University of Wisconsin
Sunil Goda is a graduate student at Stanford University
G. Y. Yin is a research scientist at Stanford University
Steve Harris is a professor at Stanford University